Supplementary Figure legends

Fig. S1: Integration of p97 interactions from selected literature

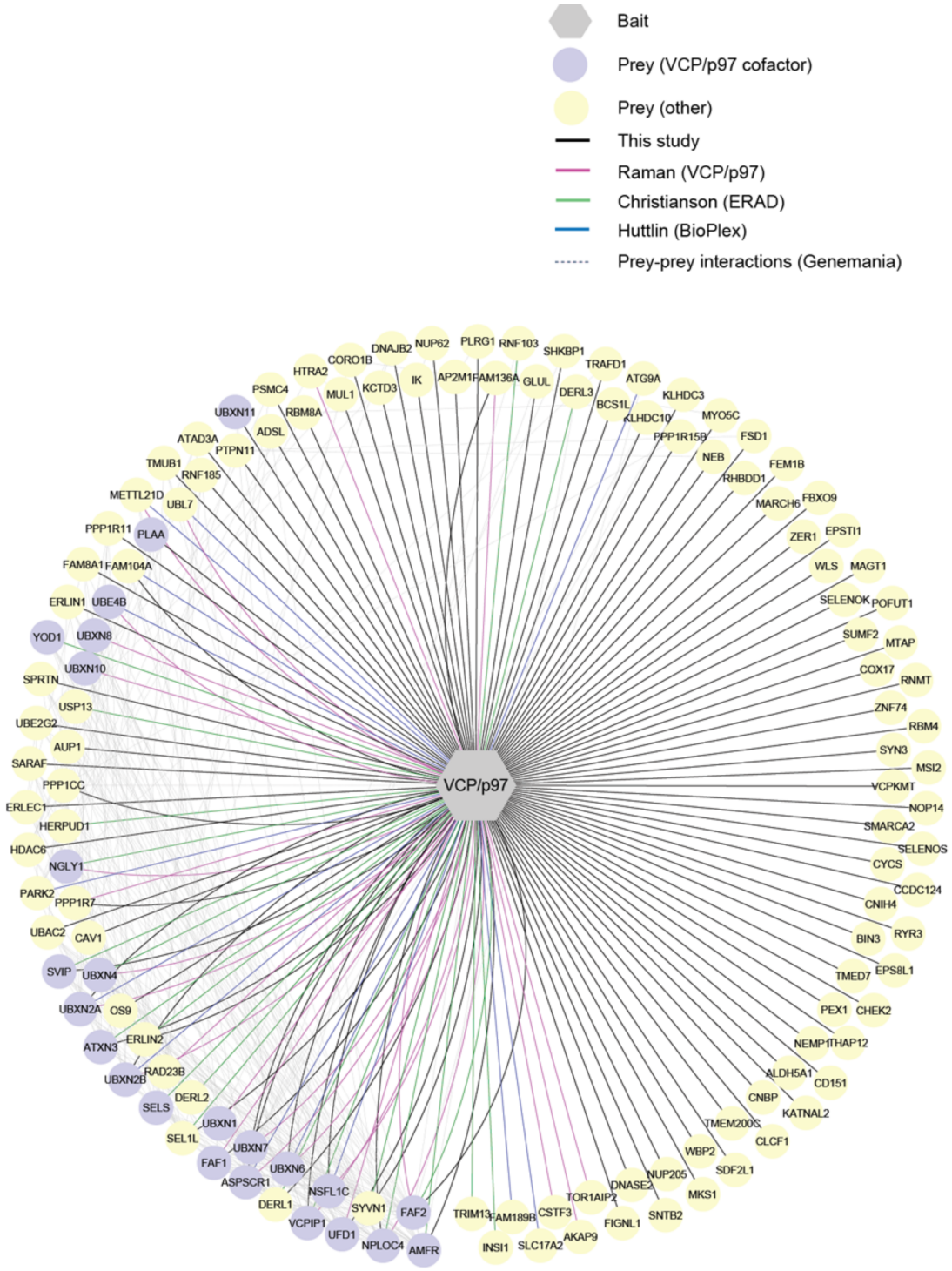

The network graph depicts p97 interactions from this study (black edges) and selected literature including the p97 adapter network from Raman *et al.* (pink edges), the ERAD network from Christianson *et al.* (green edges), and the BioPlex v2.0 network from Huttlin et al. (blue edges). Prey-prey interactions (light grey dotted lines) were retrieved from Genemania.org. The interacting proteins are arranged in a degree sorted circle i.e. prey proteins with the most interactions (including prey-prey) are at the bottom and the degree decreases in the clockwise direction starting from AMFR. VCP/p97 cofactors are defined as proteins containing established VCP/p97 interaction domains or motifs.

Fig. S2: Localization of overexpressed MUL1, RNF185 and UBE4B

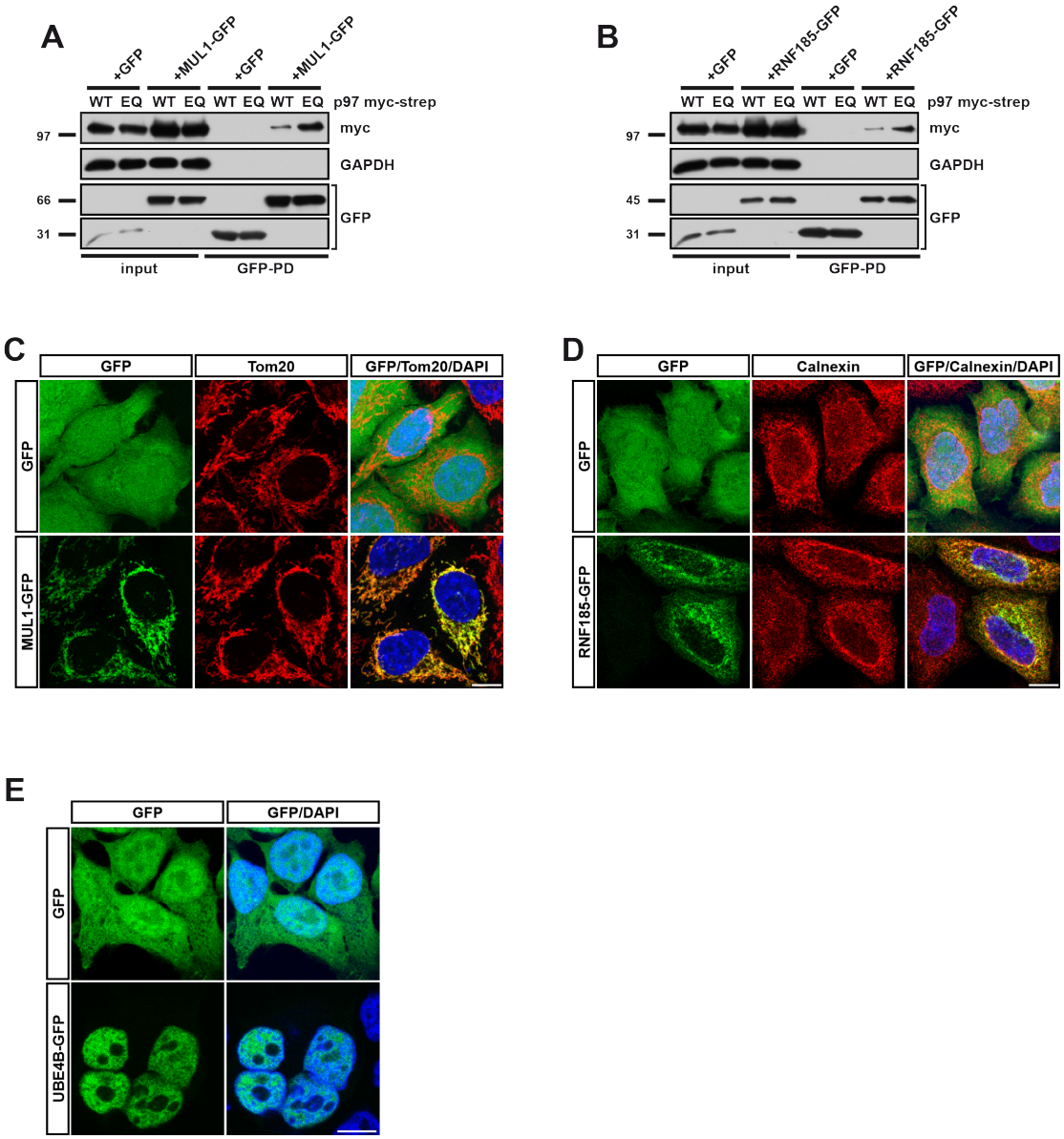

(A and B) Recapitulation of p97-E578Q trapping in HeLa cells. MUL1-GFP and RNF185-GFP were transiently expressed in HeLa cells co-transfected with either p97-WT or p97-E578Q (EQ) as indicated and isolated using GFP-specific nanobodies. Western blots as indicated.

(C and D) GFP, MUL1-GFP or RNF185-GFP were expressed in HeLa cells as indicated. Cells were fixed, and Tom20 or Calnexin were immunostained as markers for mitochondria or ER, respectively. Nuclei were stained by DAPI. Visualization by LSM confocal microscopy.

(E) Localization of GFP or UBE4B-GFP in HEK293 cells was confirmed by LSM confocal microscopy. Scale bars, 10 µm.

Fig. S3: SWATH profiles for CReP/PPP1R15B peptide ELGSSPSGPLNIQR

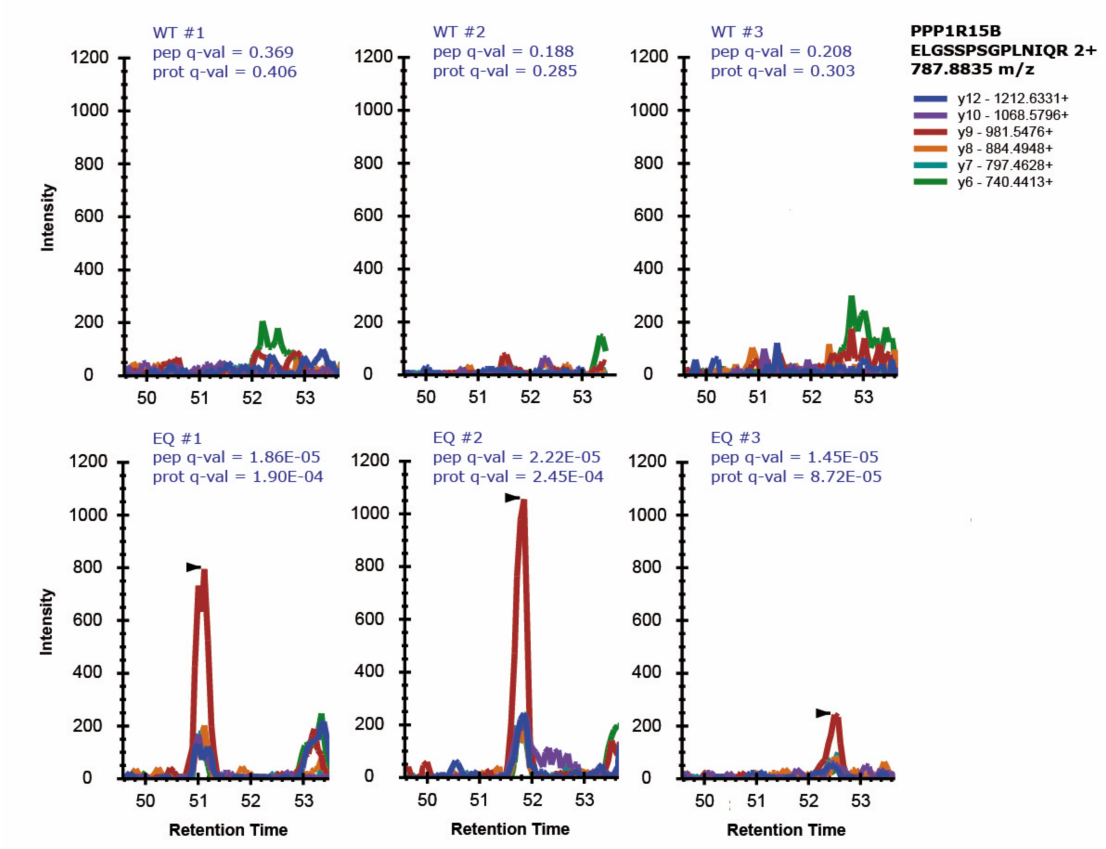

Fragment ion extracted ion chromatography from SWATH MS data of the CReP/PPP1R15B proteotypic peptide ELGSSPSGPLNIQR from three independent experiments for p97-WT and p97-EQ isolations as indicated. Note that the peptide is consistently detectable in the p97-EQ condition with protein detection q-values in the range of 10-4 to 10-5 but undetectable in the p97-WT condition.

Fig. S4: Control experiments for the analysis of CReP.

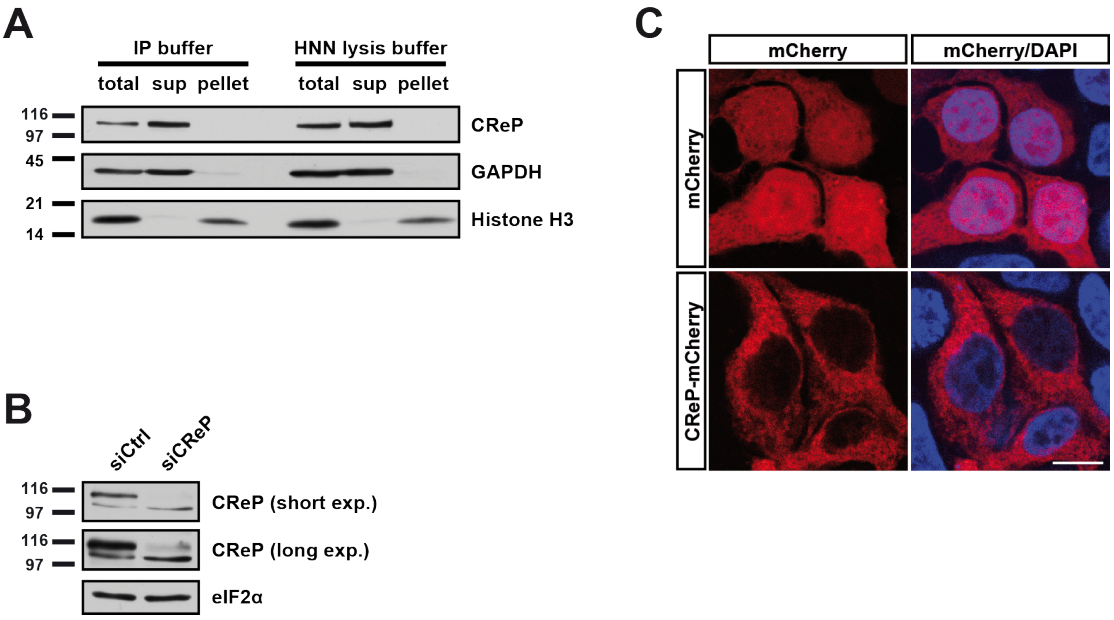

(A) Verification of efficient extraction of CReP in the buffer used for AP-MS (HNN lysis buffer) and co-immunoprecipitations (IP buffer). HEK293 cells were treated in extraction buffer. Total lysate (total) was separated by a 17,000 g centrifugation for 15 min into insoluble material (pellet) and supernatant (sup), which was used for the experiments. Endogenous CReP as well as fractionation markers (GAPDH (sup); Histone H3 (pellet)) were probed with antibodies.

(B) Verification of CReP Western blot signals. HEK293 cells were treated with control or CReP-specific siRNA for 28 hours. Lysates were immunoblotted and probed with CReP and eIF2α (loading control) antibodies. Note that two bands are recognized by the CReP antibody, but only the upper band was specifically reduced upon CReP depletion.

(C) mCherry or CReP-mCherry were transiently expressed in HEK293 cells and visualized by confocal microscopy. Nuclei were stained by DAPI. Scale bar, 10 µm.

Fig. S5: Confirmation of the effect on CReP degradation with an alternative Ufd1 siRNA.

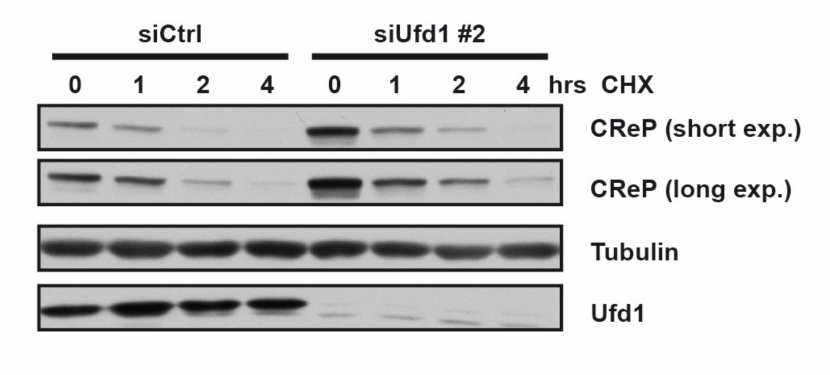

CHX chase experiment as in Fig. 4E. Note the increase in CReP steady-state levels after treatment with Ufd1 siRNA over 48 h, and delayed degradation after CHX addition. Ufd1 depletion efficiency was confirmed with a specific antibody. Tubulin was probed as loading control. Cells at time point 0 were mock (DMSO) treated.

Fig. S6: CReP degradation upon diverse stresses and effect of p97 inhibition.

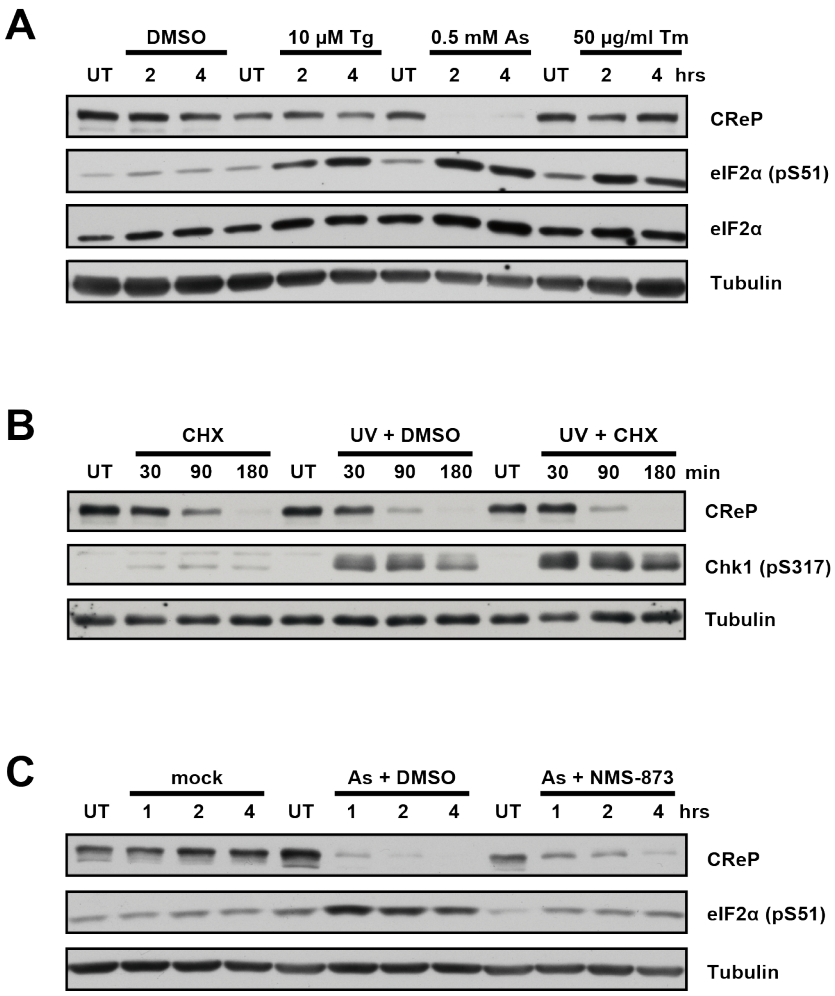

(A) Cells were treated with vehicle alone (DMSO), thapsigargin (Tg), arsenite (As), or tunicamycin (Tm). CReP levels and eIF2α phosphorylation was monitored with specific antibodies. Total eIF2α and Tubulin was probed as loading control. Note quantitative removal of CReP upon arsenite treatment and increase in eIF2α phosphorylation.

(B) Comparison of constitutive and stress-induced CReP degradation rates. Cells were treated with cycloheximide (CHX), UV, or a combination. Lysates were probed with indicated antibodies.

(C) CReP degradation upon arsenite treatment is delayed upon p97 inhibition. Experiment as in (A). Cells were treated with sodium arsenite (0.5 mM) in the absence or presence of the p97 inhibitor NMS-873 (5 µM). Note the decreased

eIF2α phosphorylation, when CReP degradation is blocked by NMS-873. UT = untreated.

Supplementary Tab. 1

Complete proteomic dataset from AP-SWATH MS acquired for p97-WT, p97-EQ, and GFP control purifications. Targeted analysis based on a spectral library containing coordinates for 3,839 proteins generated a quantitative data matrix containing 1,937 proteins. For contaminant filtering log2 fold change > 2 and p-value < 0.05 between either p97-WT or p97-EQ and GFP controls was considered a significant interaction, resulting in 108 high-confidence interactions. For mutant comparison log2 fold change > 2 or < 2 and p-value < 0.05 was considered a significant change in the interaction of a protein with p97. Note, of the 108 high confidence interacting proteins, 43 displayed an increase in binding to p97-EQ while 8 were reduced compared to p97-WT.

Supplementary Tab. 2

Data corresponding to the supplementary Fig. S1 where p97 interactions detected in previous selected studies is integrated with p97 interactions from this study.